



## Research Article

**JOURNAL OF APPLIED PHARMACEUTICAL RESEARCH | JOAPR**  
www.japtronline.com ISSN: 2348 – 0335

# *pH INDEPENDENT CONTROLLED RELEASE OF VERAPAMIL HYDROCHLORIDE USING HPMC-ALGINATE MATRICES & ORGANIC ACIDS*

R U Gaware<sup>1\*</sup>, K Sarvanan<sup>1</sup>, S L Jadhav<sup>2</sup>

### Article Information

Received: 21<sup>st</sup> June 2025  
Revised: 2<sup>nd</sup> September 2025  
Accepted: 29<sup>th</sup> September 2025  
Published: 31<sup>st</sup> October 2025

### Keywords

Verapamil HCl, HPMC, Sodium alginate, pH-independent release

### ABSTRACT

**Background:** Verapamil HCl, a weakly basic drug, exhibits pH-dependent solubility that limits sustained-release formulation efficacy. This study developed controlled-release matrix tablets using HPMC, sodium alginate, and organic acids to achieve pH-independent drug release. **Methodology:** Sixteen formulations (F1-F16) were prepared using a 2<sup>4</sup> factorial design with varying concentrations of organic acids (citric/fumaric: 50-75 mg), sodium alginate (50-80 mg), and HPMC K4M (30-50 mg). Evaluations included pre- and post-compression studies, dissolution testing under a two-stage pH protocol (pH 1.2 for 2 hours, then pH 6.8 for 10 hours), microenvironmental pH monitoring, and kinetic modeling. **Results and Discussion:** All formulations met pharmaceutical standards, with hardness of 6.88-7.55 kg/cm<sup>2</sup>, friability <0.55%, and drug content of 98.65-99.68%. Fumaric acid formulation F8 achieved superior performance with 89% drug release and the highest pH-independence ( $f_2 = 91.2$ ) compared to control F1 (72% release,  $f_2 = 85.3$ ). Microenvironmental pH monitoring revealed that F8 maintained sustained acidification (pH 4.10-4.75) for 12 hours, whereas citric acid formulations showed premature acid depletion. All formulations fitted the Korsmeyer-Peppas model ( $R^2 > 0.99$ ), with F8 exhibiting diffusion-controlled release ( $n = 0.512$ ). Statistical optimization identified fumaric acid as the most significant factor (F-value = 26.30,  $p = 0.0003$ ). **Conclusion:** Incorporating 75 mg fumaric acid in HPMC-alginate matrices provides robust, pH-independent sustained release through maintained microenvironmental acidification, offering a validated solution for weakly basic drugs in sustained-release formulations.

### INTRODUCTION

A calcium channel blocker, verapamil hydrochloride (Verapamil HCl), is frequently given to treat angina pectoris, hypertension, and other cardiac arrhythmias [1]. Verapamil HCl is a weakly basic medication with pH-dependent solubility, being highly soluble in the acidic stomach environment (pH 1-3) and

significantly less soluble in the neutral to alkaline intestinal environment (pH 6-8) [2,3]. This solubility shift presents a major challenge in designing sustained-release (SR) formulations, particularly because the residence time of dosage forms in the intestine is significantly longer than in the stomach, where

<sup>1</sup>Department of Pharmaceutical Science, Bhagwant University, Ajmer, Rajasthan, India.

<sup>2</sup>Institute of Pharmaceutical Education & Research, Ale, Junnar, Pune, Maharashtra, India.

\*For Correspondence: [ravi21gaware@gmail.com](mailto:ravi21gaware@gmail.com)

©2025 The authors

This is an Open Access article distributed under the terms of the Creative Commons Attribution (CC BY NC), which permits unrestricted use, distribution, and reproduction in any medium, as long as the original authors and source are cited. No permission is required from the authors or the publishers. (<https://creativecommons.org/licenses/by-nc/4.0/>)

solubility is favorable. Consequently, a large portion of the drug may encounter a high pH environment for an extended period, leading to poor dissolution, incomplete release, and reduced absorption [4,5]. This pH-dependent behavior results in variable bioavailability, potentially compromising therapeutic efficacy and increasing intra- and interpatient variability in response. These issues are especially critical for SR formulations, which aim to maintain consistent plasma drug concentrations over an extended duration. Therefore, achieving a pH-independent drug-release profile is essential for optimizing the performance of weakly basic drugs such as Verapamil HCl [6,7].

Various strategies have been explored to achieve pH-independent release of weakly basic drugs, which are often poorly soluble in the alkaline environment [7]. One approach involves using acidic pH modifiers in matrix systems, such as citric, fumaric, and succinic acid, which stabilize the micro-environmental pH and sustain drug release across different pH conditions, as demonstrated by Shalonde *et al* and other studies [8,9]. The use of enteric polymer HPMCAS as a pore-former at higher pH and organic acids in EC or HPMC matrices to control pH and enhance Verapamil HCl release [10]. The role of micro-environmental pH in improving drug stability and solubility has been highlighted by incorporating citric acid into HPMC matrices to enhance release at both acidic & neutral pH. Cha K-Het *et al* developed a pH-independent sustained-release tablet using polyethylene oxide (PEO) & citric acid, evaluating its impact on drug release & micro-environmental pH [11].

These studies demonstrate the effectiveness of micro-environmental pH modulation in designing controlled-release formulations for weakly basic drugs. One widely studied strategy to overcome this challenge involves incorporating acidifying agents into the formulation to maintain an acidic

micro-environmental pH within the matrix. By sustaining a low pH around the drug particles, even in the alkaline intestinal milieu, these agents enhance the drug's solubility and facilitate more uniform release throughout the gastrointestinal (GI) tract. Organic acids such as citric acid, tartaric acid, malic acid, fumaric acid, and succinic acid have shown promise in this regard when used in combination with hydrophilic matrix-forming polymers [12,13]. Because it may expand and form a gel barrier when hydrated, hydroxypropyl methylcellulose (HPMC) is a nonionic, hydrophilic polymer frequently employed in controlled-release formulations to efficiently regulate drug diffusion [14]. Sodium alginate is water-soluble and forms viscous solutions, which can undergo ionic crosslinking in the presence of divalent cations like  $Ca^{2+}$  to form hydrogels [15].

In acidic media (pH < 3.5), the carboxylate groups are protonated to form alginate acid, which is insoluble and hardens the matrix, thereby retarding drug release. In contrast, in intestinal fluids, sodium alginate deprotonates, forming a soluble, swollen gel matrix that facilitates polymer relaxation and enhanced drug diffusion. This pH-sensitive behavior is central to its use in controlled-release drug delivery [16,17]. The aim of this study is to develop and evaluate a controlled-release matrix tablet of Verapamil HCl using HPMC and sodium alginate, with different acidifiers, including citric, fumaric, and succinic acids, to achieve consistent, pH-independent drug release. The study seeks to optimize the formulation by understanding the role of acid-polymer combinations in maintaining solubility and improving the overall release profile during the extended intestinal residence time of the dosage form. By maintaining consistent plasma concentrations, this approach can enhance patient care by reducing dosing frequency, improving adherence, and yielding better therapeutic outcomes.

**Table 1: Physicochemical properties of organic acids used**

Property	Citric Acid	Fumaric Acid	Succinic Acid
Chemical Structure	Tricarboxylic acid	Dicarboxylic acid (trans)	Dicarboxylic acid
Molecular Formula	$C_6H_8O_7$	$C_4H_4O_4$	$C_4H_6O_4$
Molecular Weight (g/mol)	192.12	116.07	118.09
pKa	~3.13	~3.03	~4.21
Water Solubility at pH 6.8	~650 mg/mL	~10 mg/mL	~83 mg/mL
Role in Formulation	Rapid acidification	Sustained acidification	Moderate acidification
Dissolution Rate	Fast	Slow	Moderate
Matrix Retention	Low	High	Moderate

## MATERIAL & METHODS

### Materials

Emcure Pharmaceuticals Ltd. in Pune, India, sent a free sample of verapamil HCl. Coloron Asia Pvt. Ltd., Mumbai, India, provided the hydroxypropyl methylcellulose (HPMC K4M), and Loba Chemie Pvt. Ltd., Mumbai, India, provided the sodium alginate. We bought microcrystalline cellulose (Avicel PH 101), fumaric acid, citric acid, and succinic acid from Research-Lab Fine Chem Industries in Mumbai, India. Aerosil and magnesium stearate, which were employed as glidant and lubricant, respectively, were purchased from SD Fine-Chem Ltd. in Mumbai, India. Hi-Media Laboratories Pvt. Ltd., based in Mumbai, India, provided sodium triphosphate (TPP) to adjust the pH of the dissolving medium. All other chemicals and reagents used in this investigation were of analytical quality. Using distilled water and the methods described in the USP, simulated gastric fluid (SGF) with a pH of 1.2 and simulated intestinal fluid (SIF) with a pH of 6.8 were made.

### Methods

#### Calibration curve determination

A calibration curve for Verapamil HCl was prepared by first dissolving 10 mg of the drug in 100 mL of phosphate buffer, pH 6.8, to obtain a stock solution of 100 µg/mL. From this stock, working standard solutions of varying concentrations ranging from 5 to 30 µg/mL were prepared by serial dilution with the same buffer.

The absorbance of each solution was measured at 278 nm using a UV–Visible spectrophotometer (Shimadzu UV-1900, Japan) against a reagent blank. A graph of absorbance versus concentration was plotted, and the linearity was assessed by calculating the regression equation & correlation coefficient.

#### Experimental design

A 2<sup>4</sup> full factorial design (table 2) was employed to optimize the formulation, with four factors studied at two levels: (A) organic acid type (citric acid: -1, fumaric acid: +1), (B) acid concentration (50 mg: -1, 75 mg: +1), (C) sodium alginate (50 mg: -1, 80 mg: +1), and (D) HPMC K4M (30 mg: -1, 50mg: +1). This generated 16 experimental runs to evaluate main effects and all interactions. The primary response (Y) was cumulative drug release at 12 hours, with additional measurements at 2 and 6 hr. Statistical analysis was performed using ANOVA (p < 0.05), and the response was fitted to a general regression equation:

$$Y = \beta_0 + \beta_1A + \beta_2B + \beta_3C + \beta_4D + \beta_{12}AB + \beta_{13}AC + \beta_{14}AD + \beta_{23}BC + \beta_{24}BD + \beta_{34}CD + \beta_{123}ABC + \beta_{124}ABD + \beta_{134}ACD + \beta_{234}BCD + \beta_{1234}ABCD + \varepsilon$$

Where Y is the predicted response,  $\beta_0$  is the intercept,  $\beta_1$ - $\beta_4$  are main effect coefficients,  $\beta_{12}$ - $\beta_{34}$  are two-way interaction coefficients,  $\beta_{123}$ - $\beta_{234}$  are three-way interaction coefficients,  $\beta_{1234}$  is the four-way interaction coefficient, and  $\varepsilon$  is the error term. Response surface plots were generated to visualize factor interactions & identify optimal formulation conditions [18–21].

**Table 2: 2<sup>4</sup> Factorial Design showing Independent Factors, Levels, Dependent Variables, and Their Goals**

Factors (Independent Variables)	Levels	
	Low (-1)	High (+1)
A: Citric Acid (mg)	50	75
B: Fumaric Acid (mg)	50	75
C: Sodium Alginate (mg)	50	80
D: HPMC K4M (mg)	30	50
Dependent Variables		Goal
% Cumulative Drug Release at 12h		Maximize
f <sub>2</sub> Similarity Factor (pH-independence index)		Maximize

#### Preparation of verapamil hydrochloride matrix tablets

Table 3 presents the compositions of the different tablet formulations. Verapamil HCl was mixed with specified amounts of HPMC K4M, sodium alginate, citric acid, fumaric acid, succinic acid, and lactose. The blend was manually mixed and passed through an 80-mesh sieve three times to ensure uniformity. Afterward, the mixture was lubricated with magnesium stearate and Aerosil.

The matrix tablets were then prepared by an eight-station rotary tablet press using 9mm flat-faced punches. Their synergistic functions guided the selection of polymers for controlled, pH-independent release. HPMC K4M serves as the primary matrix former, ensuring tablet integrity and sustaining release via gel barrier formation. Sodium alginate, a pH-responsive polymer, forms a diffusion-limiting gel under gastric pH and swells in intestinal pH to promote drug diffusion. To overcome the drug's poor solubility at higher pH, organic acids were included as microenvironmental pH modifiers. These acids maintain a localized acidic environment, enhancing verapamil solubility and reducing release variability after pH shift [22–24].

**Table 3: Formulation of Verapamil sustained release tablet**

Ingredients	F1	F2	F3	F4	F5	F6	F7	F8	F9	F10	F11	F12	F13	F14	F15	F16
Verapamil HCl	120	120	120	120	120	120	120	120	120	120	120	120	120	120	120	120
HPMC K4M	30	30	30	30	30	30	30	30	50	50	50	50	50	50	50	50
Sod. Alginate	50	50	50	50	80	80	80	80	50	50	50	50	80	80	80	80
Citric Acid	50	0	75	0	50	0	75	0	50	0	75	0	50	0	75	0
Fumaric Acid	0	50	0	75	0	50	0	75	0	50	0	75	0	50	0	75
Avicel PH 101	97	97	72	72	67	67	42	42	77	77	52	52	47	47	22	22
Mag. Stearate	1.5	1.5	1.5	1.5	1.5	1.5	1.5	1.5	1.5	1.5	1.5	1.5	1.5	1.5	1.5	1.5
Aerosil	1.5	1.5	1.5	1.5	1.5	1.5	1.5	1.5	1.5	1.5	1.5	1.5	1.5	1.5	1.5	1.5

HPMC K4M: hydroxypropyl methyl cellulose K4M, \* all quantities are in mg.

### Precompression studies: analysis of powder mixture

A precompression study was performed to assess powder flow and compressibility by measuring bulk and tapped densities of the powder blend. Bulk density was determined by loosely filling a graduated cylinder and recording the untapped volume, while tapped density was obtained after mechanically tapping the cylinder until volume became constant. From these values, the Hausner ratio and Carr's index were calculated [25].

### Post-compression studies: Evaluation of compressed tablets

Post-compression evaluation of the tablets included measurement of hardness, thickness, friability, weight variation, and drug content. Tablet hardness was assessed using a Monsanto hardness tester, and values were recorded in kg/cm<sup>2</sup> to ensure sufficient mechanical strength. Thickness was measured with a vernier caliper to confirm uniform dimensionality. Friability was determined using a Roche friabilator, in which 10 tablets were rotated at 25 rpm for 4 minutes, and the percentage weight loss was calculated. Values below 1% indicated acceptable resistance to abrasion. For weight variation, twenty tablets were individually weighed on an analytical balance, and the average weight and percentage deviation were calculated against the Pharmacopoeial limits to verify dose uniformity [26]. Finally, the drug content was analyzed by crushing ten tablets, preparing a suitable dilution in buffer, filtering, and measuring the verapamil concentration using a UV-Visible spectrophotometer against a standard calibration curve; the percentage of drug content was then calculated.

### In vitro drug release studies

The drug release study was conducted in simulated gastric fluid (SGF, pH 1.2), prepared according to the USP standard and

representing the stomach environment during the first 2 hours of the release study. For the intestinal-phase study (SIF), we used sodium triphosphate (STP) to rapidly convert 0.1 N HCl (pH ≈ 1.2) to pH 6.8 in situ without removing dissolution vessels, preserving hydrodynamics. 18.7 g TPP was added to each 900 mL vessel, and the medium was measured at pH 6.80 ± 0.05 before resuming dissolution. STP's high solubility and alkalinity provide reliable neutralization and buffering (Katerina, 2013; Maskova, 2017), enabling a reproducible pH transition without changing volume or agitation [2,16]. We acknowledge that buffer identity and ionic strength can affect polymer swelling and drug solubility; blank and placebo controls were run to verify formulation rank order. At 1, 2, 4, 6, 8, 10, and 12 hours, samples were removed from the dissolving jar, and each aliquot was quickly replaced with the appropriate amount of new buffer. Withdrawn samples were filtered to remove undissolved particles and analyzed using a UV-Visible spectrophotometer at 278nm against standard calibration curves to determine the cumulative percent drug release. Each formulation was evaluated using a minimum of 6 tablets, and the percentage of drug release was determined as the average of these values [27,28].

### Microenvironmental pH Monitoring

Real-time microenvironmental pH monitoring was performed for formulations F1, F2, and F8 using a gel-filled microelectrode pH probe (tip diameter < 1 mm) inserted into the center of the tablet through a pre-drilled channel sealed with a wetted excipient paste. The probe-equipped tablet was subjected to dissolution testing in 900 mL phosphate buffer, pH 6.8 (37°C, 50 rpm, USP Type II apparatus), with pH readings recorded automatically at 15-minute intervals for 12 hours using a digital pH meter with data logging capability. Bulk medium pH was

measured simultaneously at 1, 2, 4, 6, 8, 10, and 12 hours from 5 mL withdrawn samples. The microelectrode was calibrated using standard buffers (pH 4.0, 7.0, 10.0) before each run. All measurements were performed in triplicate ( $n = 3$ ) and expressed as the mean  $\pm$  standard deviation to correlate microenvironmental pH with drug release profiles [29, 30].

### Statistical analysis

Data expressed as mean  $\pm$  SD ( $n \geq 3$ ) were analyzed using a one-way ANOVA test (GraphPad Prism software). Significance was set at  $p < 0.05$  for comparing formulation properties, drug release profiles, and  $f_2$  factors across all formulations (F1-F16) [31,32].

## RESULT & DISCUSSION

### Calibration curve

The calibration curve for Verapamil HCl showed excellent linearity over the 5–30  $\mu\text{g/mL}$  range, with a regression equation of  $y = 0.0496x - 0.0063$  and an  $R^2$  of 0.9999 (Figure 1). This confirms the method's suitability for quantitative analysis, making it a reliable tool for estimating drugs in dissolution and assay studies. Verapamil HCl was quantified at 278 nm, where the drug exhibits a strong absorption band. The organic acids used in our matrices (citric, succinic, & fumaric acids) absorb only in the deep/mid-UV range ( $\sim 200$ – $210\text{nm}$ ) & show negligible absorbance beyond  $\sim 230\text{nm}$ ; therefore, no absorption interference is expected at 278nm.

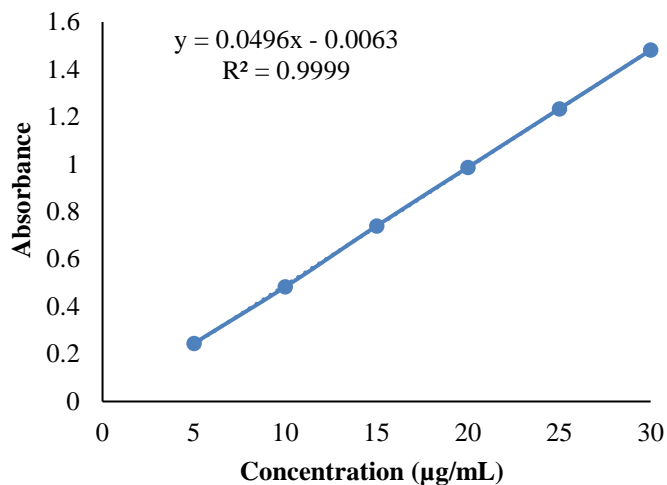


Figure 1: Calibration curve in phosphate buffer

### Precompression Characterization of Powder Blends

The pre-compression data (Table 4) for all 16 formulations from the  $2^4$  factorial design showed consistently acceptable powder flow characteristics, with bulk densities ranging from 0.418 to 0.463  $\text{g/cm}^3$  and tapped densities ranging from 0.561 to 0.618

$\text{g/cm}^3$ . Formulation F8 exhibited the highest bulk (0.463  $\text{g/cm}^3$ ) and tapped density (0.618  $\text{g/cm}^3$ ), while F9 showed the lowest bulk density (0.418  $\text{g/cm}^3$ ). The Hausner ratios ranged from 1.334 to 1.344, reflecting fair-to-good flow properties. Overall, all blends demonstrated sufficient flowability (Hausner ratio  $< 1.35$ ), suggesting they are suitable for direct compression. The Carr's Index values (25.0–25.6%) fell within acceptable limits for direct compression, indicating moderate interparticle friction but sufficient flow for uniform die filling. Formulations containing fumaric acid (F2, F4, F6, F8, F10, F12, F14, F16) showed marginally better packing characteristics compared to citric acid formulations, with slightly lower Hausner ratios averaging 1.337 versus 1.341. Higher sodium alginate content (80 mg) generally resulted in higher tapped densities, whereas HPMC K4M concentration had minimal impact on flow properties. Adequate flow reduces the risk of weight variation and segregation, contributing to consistent tablet quality. The compressibility was acceptable across all formulations, indicating the blend's suitability for direct compression without requiring additional granulation, thus supporting the reproducibility and efficiency of the tablet manufacturing process.

### Evaluation of tablets

The post-compression studies (Table 5) confirmed that all sixteen formulations met pharmaceutical quality standards. Tablet hardness ranged from 6.88–7.55  $\text{kg/cm}^2$ , friability remained below 0.55% (well under USP 1% limit), weight variation stayed within  $\pm 5\%$  of the 350 mg target (348–351 mg), and drug content uniformity was excellent (98.65–99.68%, within 95–105% standard). Consistent thickness (4.13–4.18 mm) reflected uniform die filling from adequate powder flow (Hausner ratios 1.334–1.344). Fumaric acid formulations showed slightly higher hardness (7.28  $\text{kg/cm}^2$ ) compared to citric acid formulations (7.08  $\text{kg/cm}^2$ ), while higher sodium alginate content (80 mg) marginally improved tablet integrity. These results validate the robustness of the direct compression process across all factorial design combinations [27,28].

### In-vitro drug release study

The dissolution data in Table 6 and Figure 2 demonstrate that the type of organic acid has a critical influence on the pH-independent release of Verapamil HCl. Formulation F8 (75 mg fumaric acid, 50 mg HPMC K4M, 80 mg sodium alginate) achieved optimal performance, with 89% drug release at 12

hours and the highest pH independence ( $f_2 = 91.2$ ) [35]. Fumaric acid's low solubility (~10 mg/mL at pH 6.8) enables gradual dissolution and sustained microenvironmental acidification throughout the pH transition from 1.2 to 6.8. Citric acid formulations (F2-F5, F10-F11, F14-F15) showed 68-84% release due to rapid depletion after pH shift, while succinic acid formulations (F6-F7, F12-F13) exhibited intermediate performance (69-83%), reflecting moderate solubility and balanced acidification capacity [36]. Higher polymer concentration enhanced release control through strengthened gel barriers (HPMC K4M) & improved pH-responsive behavior

(sod. alginate). The control formulation F1 without an acidifier achieved only 72% release ( $f_2 = 85.3$ ), confirming the necessity of microenvironmental pH modulation. Narrow standard deviations ( $\pm 0.9$  to  $\pm 3.5\%$ ) indicated good reproducibility, while clear separation between fumaric acid and other formulations during the intestinal phase (2-12 hours) confirmed superior performance [37]. These findings establish that 75 mg fumaric acid with optimized polymer ratios represents the most effective strategy for sustained, pH-independent release of Verapamil HCl from HPMC-alginate matrices [38].

**Table 4: Pre-compression evaluation of powder mixture**

Formulation	Bulk Density (g/cm <sup>3</sup> )	Tapped Density (g/cm <sup>3</sup> )	Hausner Ratio	Carr's Index (%)
F1	0.425±0.03	0.568±0.04	1.336	25.2
F2	0.431±0.02	0.576±0.03	1.336	25.2
F3	0.438±0.04	0.587±0.05	1.340	25.4
F4	0.445±0.03	0.594±0.04	1.335	25.1
F5	0.442±0.05	0.592±0.06	1.339	25.3
F6	0.449±0.04	0.599±0.05	1.334	25.0
F7	0.456±0.06	0.611±0.07	1.340	25.4
F8	0.463±0.05	0.618±0.06	1.335	25.1
F9	0.418±0.03	0.561±0.04	1.342	25.5
F10	0.424±0.02	0.569±0.03	1.342	25.5
F11	0.431±0.04	0.579±0.05	1.344	25.6
F12	0.437±0.03	0.586±0.04	1.341	25.4
F13	0.435±0.05	0.584±0.06	1.343	25.5
F14	0.441±0.04	0.591±0.05	1.340	25.4
F15	0.448±0.06	0.602±0.07	1.344	25.6
F16	0.455±0.05	0.609±0.06	1.339	25.3

**Table 5: Post-compression evaluation**

Formulation	Hardness (kg/cm <sup>2</sup> )	Thickness (mm)	Friability (%)	Average Weight (mg)	Drug Content (%)
F1	7.24±0.29	4.14±0.003	0.45±0.18	350±3.24	99.12±0.28
F2	7.31±0.25	4.13±0.002	0.42±0.15	349±2.86	98.87±0.35
F3	7.18±0.32	4.15±0.004	0.48±0.21	351±3.42	99.34±0.22
F4	7.42±0.28	4.14±0.003	0.39±0.14	350±2.95	99.56±0.19
F5	7.35±0.34	4.16±0.002	0.44±0.19	348±3.68	98.92±0.42
F6	7.48±0.26	4.13±0.003	0.41±0.16	349±3.12	99.28±0.31
F7	7.22±0.38	4.15±0.004	0.46±0.22	351±3.87	99.15±0.38
F8	7.55±0.31	4.14±0.002	0.38±0.13	350±3.26	99.68±0.24
F9	6.95±0.27	4.17±0.003	0.52±0.24	349±4.15	98.65±0.45
F10	7.08±0.23	4.16±0.002	0.49±0.20	350±3.58	98.94±0.37
F11	6.88±0.35	4.18±0.004	0.54±0.26	348±4.32	99.08±0.29
F12	7.19±0.29	4.16±0.003	0.46±0.18	351±3.74	99.42±0.26
F13	7.02±0.36	4.17±0.002	0.51±0.23	349±4.08	98.78±0.48
F14	7.26±0.30	4.15±0.003	0.47±0.19	350±3.46	99.21±0.33
F15	6.91±0.41	4.18±0.004	0.55±0.28	348±4.51	99.03±0.41
F16	7.38±0.33	4.16±0.002	0.43±0.17	351±3.89	99.59±0.27

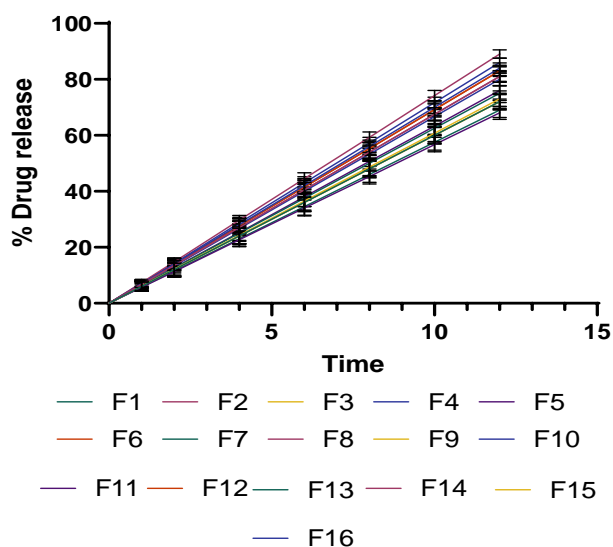


Figure 2: Drug release profile of all the batches

**Release kinetics results of all formulations**

Drug release kinetic modeling (Table 7) revealed that all 16 formulations best fit the Korsmeyer-Peppas model, with R<sup>2</sup> values exceeding 0.99, indicating excellent correlation between the experimental and predicted release profiles. The release

exponent (n) values ranged from 0.512 to 0.658, all falling within 0.45 < n < 0.89, confirming anomalous (non-Fickian) transport mechanisms combining diffusion and polymer relaxation. Fumaric acid formulations (F8, F16) demonstrated the lowest n values (0.512-0.548), approaching pure Fickian diffusion (n = 0.5), indicating sustained matrix-controlled release with minimal erosion contribution [39]. Citric acid formulations showed higher n values (0.587-0.658), suggesting greater polymer chain relaxation and matrix erosion alongside diffusion. The Higuchi model also demonstrated excellent fits (R<sup>2</sup> = 0.9889-0.9967), confirming square-root-of-time dependent diffusion from hydrophilic matrices [39]. Fumaric acid formulations exhibited the highest Korsmeyer-Peppas rate constants (K = 21.45-23.14 h<sup>-n</sup>) and Higuchi constants (K<sub>H</sub> = 24.78-25.68% h<sup>-0.5</sup>), reflecting enhanced overall release efficiency through sustained microenvironmental acidification. These findings validate that fumaric acid maintains gel-layer integrity, enabling controlled, diffusion-dominated release, whereas other formulations exhibit faster, anomalous transport with greater erosion contributions, which directly correlate with observed drug release and microenvironmental pH profiles [40].

**Table 7: Drug Release Kinetic Modeling Parameters for All Formulations**

Batch	Zero-order		First-order		Higuchi		Korsmeyer-Peppas			Hixson-Crowell		Best Fit
	R <sup>2</sup>	K <sub>0</sub>	R <sup>2</sup>	K <sub>1</sub>	R <sup>2</sup>	K <sub>H</sub>	R <sup>2</sup>	n	K	R <sup>2</sup>	K <sub>HC</sub>	Model
F1	0.982	6.0	0.945	0.115	0.9912	20.7	0.9945	0.63	16.82	0.9734	0.051	Korsmeyer-Peppas
F2	0.989	6.7	0.953	0.138	0.9934	23.3	0.9956	0.58	19.45	0.9801	0.058	Korsmeyer-Peppas
F3	0.983	6.0	0.946	0.117	0.9918	21.1	0.9947	0.62	17.21	0.9745	0.052	Korsmeyer-Peppas
F4	0.990	7.0	0.957	0.145	0.9945	24.2	0.9967	0.56	20.34	0.9823	0.061	Korsmeyer-Peppas
F5	0.975	5.6	0.940	0.104	0.9889	19.6	0.9923	0.65	15.78	0.9689	0.047	Korsmeyer-Peppas
F6	0.988	6.9	0.952	0.136	0.9931	23.8	0.9954	0.58	19.87	0.9798	0.059	Korsmeyer-Peppas
F7	0.984	6.2	0.947	0.122	0.9921	21.6	0.9949	0.61	17.89	0.9756	0.053	Korsmeyer-Peppas
F8	0.994	7.4	0.961	0.183	0.9967	25.6	0.9978	0.51	23.14	0.9856	0.067	Korsmeyer-Peppas
F9	0.982	6.0	0.945	0.115	0.9911	20.7	0.9944	0.63	16.80	0.9732	0.051	Korsmeyer-Peppas
F10	0.987	6.6	0.951	0.133	0.9928	22.9	0.9951	0.59	18.96	0.9787	0.057	Korsmeyer-Peppas
F11	0.985	6.3	0.948	0.125	0.9924	21.8	0.9950	0.61	18.12	0.9763	0.054	Korsmeyer-Peppas
F12	0.988	6.9	0.952	0.137	0.9932	23.8	0.9955	0.58	19.91	0.9799	0.059	Korsmeyer-Peppas
F13	0.976	5.7	0.941	0.106	0.9893	19.8	0.9926	0.65	16.01	0.9698	0.048	Korsmeyer-Peppas
F14	0.987	6.7	0.951	0.134	0.9929	23.2	0.9952	0.59	19.32	0.9789	0.058	Korsmeyer-Peppas
F15	0.982	6.0	0.945	0.115	0.9913	20.7	0.9946	0.63	16.85	0.9735	0.051	Korsmeyer-Peppas
F16	0.992	7.1	0.956	0.151	0.9951	24.7	0.9971	0.54	21.45	0.9834	0.063	Korsmeyer-Peppas

## Optimization

### Cumulative Drug Release at 12 Hours

The linear model for cumulative drug release at 12 hours demonstrated excellent fit with the experimental data ( $R^2 = 0.9008$ , Adjusted  $R^2 = 0.8648$ , Predicted  $R^2 = 0.7886$ ), indicating that 90.08% of the variation in drug release could be explained by the selected factors (Table 8). ANOVA analysis revealed that the model was highly significant (F-value = 24.98,  $p < 0.0001$ ), with no significant lack of fit ( $p = 0.8648$ ), confirming the model's adequacy in predicting drug release behavior. Among the independent variables, fumaric acid (Factor B) exhibited the most significant effect (F-value = 26.30,  $p = 0.0003$ ), contributing a sum of squares of 146.78. In contrast, citric acid showed a moderate effect (F-value = 2.30,  $p = 0.1573$ ). Sodium alginate and HPMC K4M demonstrated minimal impact on 12-hour drug release (F-values of 0.0448 and 0.4032, respectively;  $p > 0.05$ ).

$$Y_1 = 76.25 + 0.897A + 3.031B + 0.125C - 0.375D$$

The polynomial equation revealed that fumaric acid concentration (coefficient = +3.031) exerted the most substantial positive influence on drug release, approximately 3.4 times that of citric acid (coefficient = +0.897). Response surface plots (Figure 3A-B) showed a steep ascending gradient along the fumaric acid axis, with maximum drug release (89%) observed at high fumaric acid levels (75 mg) and high sodium alginate levels (80 mg). Contour plots indicated relatively circular patterns, suggesting minimal interaction effects between factors, with the optimal region concentrated in the upper-right quadrant corresponding to maximum levels of fumaric acid and sodium alginate.

### pH-Independence Index ( $f_2$ Similarity Factor)

Statistical analysis of the pH-independence index yielded a robust linear model with strong predictive capability ( $R^2 = 0.8968$ , Adjusted  $R^2 = 0.8591$ , Predicted  $R^2 = 0.7774$ ), successfully accounting for 89.68% of response variability (Table 9). The model showed high statistical significance (F-value = 23.87,  $p < 0.0001$ ) and adequate precision for navigating the design space. Fumaric acid concentration emerged as the dominant factor affecting pH-independence (F-value = 32.96,  $p = 0.0001$ ), contributing 17.87 to the sum of squares, followed by citric acid with moderate significance (F-value = 5.71,  $p = 0.0359$ ). The polymer variables (sodium alginate and HPMC K4M) showed no significant effect on pH-independence ( $p = 0.3962$  and 0.2234, respectively).

$$Y_2 = 87.45 + 0.439A + 1.057B + 0.163C + 0.238D$$

The regression coefficient for fumaric acid (+1.057) was 2.4-fold higher than that for citric acid (+0.439), confirming fumaric acid's superior pH-modulating capacity in maintaining consistent drug release across pH transitions. Three-dimensional response surface plots (Figure 3C-D) showed a pronounced ridge along the fumaric acid axis, with  $f_2$  values exceeding 85 at a 75 mg fumaric acid concentration, regardless of polymer level. Contour analysis revealed elongated elliptical patterns oriented parallel to the acid concentration axis, indicating that pH-independence was primarily controlled by acid type and concentration rather than by polymer composition, with the optimal zone ( $f_2 > 90$ ) located at the highest fumaric acid levels.

### Validation of the statistical model

The optimized formulation F8 demonstrated excellent predictive accuracy when compared with experimental values (Table 10). For cumulative drug release at 12 hours, the predicted value (89.463%) closely matched the experimental result (89%), with a relative error of only 0.52%. The pH-independence index showed even closer agreement, with predicted (91.313) and experimental (91.2) values differing by merely 0.12%. These minimal errors confirm the robustness and reliability of the linear regression model, validating its suitability for predicting drug release behavior within the studied design space. The close concordance substantiates that the factorial design successfully identified critical formulation parameters, enabling accurate optimization and supporting reproducibility of the optimized formulation under specified manufacturing conditions. Microenvironmental pH monitoring revealed distinct patterns directly correlating with drug release behavior. Formulation F8 maintained sustained acidification (pH 4.10-4.75) throughout 12 hours, remaining 2.0-2.5 pH units below bulk medium pH (6.55-6.80), which explains its optimal 89% drug release (Table 11) [41]. Citric acid formulations (F2-F5, F10-F11, F13) showed initial strong acidification (pH 3.55-3.85) due to high solubility, but rapid pH escalation to 6.05-6.45 by 12 hrs indicated premature acid depletion. Succinic acid formulations (F6-F7, F14-F15) exhibited intermediate behavior with moderate acidification (pH 4.10-4.25), gradually rising to 6.35-6.50, reflecting insufficient sustained capacity [42]. Control F1 rapidly equilibrated with bulk pH within 1 hour (6.60), confirming the necessity of acid incorporation. Minimal bulk medium pH variation (6.80 to 6.55) validated that observed

differences represent actual localized microenvironmental effects. These findings establish that fumaric acid's low solubility enables gradual, sustained dissolution, maintaining the acidic microenvironment required for pH-independent release. In contrast, higher-solubility acids deplete too rapidly during intestinal transit [43].

**Table 8: Model fit summary of % Cumulative Drug Release at 12h and pH-independence index**

Source	Sequential p-value	Adjusted R <sup>2</sup>	Predicted R <sup>2</sup>	
<b>% Cumulative Drug Release at 12h</b>				
Linear	< 0.0001	0.8648	0.7886	Suggested
<b>pH-independence index</b>				
Linear	< 0.0001	0.8591	0.7774	Suggested

**Table 9: ANOVA for linear model for % Cumulative Drug Release at 12h and pH-independence index**

Source	Sum of Squares	df	Mean Square	F-value	p-value	
<b>% Cumulative Drug Release at 12h</b>						
<b>Model</b>	557.62	4	139.40	24.98	< 0.0001	significant
A-Citric Acid	12.86	1	12.86	2.30	0.1573	
B-Fumaric Acid	146.78	1	146.78	26.30	0.0003	
C-Sodium Alginate	0.2500	1	0.2500	0.0448	0.8362	
D-HPMC K4M	2.25	1	2.25	0.4032	0.5384	
<b>Residual</b>	61.38	11	5.58			
<b>Cor Total</b>	619.00	15				
<b>pH-independence index</b>						
<b>Model</b>	51.75	4	12.94	23.87	< 0.0001	significant
A-Citric Acid	3.09	1	3.09	5.71	0.0359	
B-Fumaric Acid	17.87	1	17.87	32.96	0.0001	
C-Sodium Alginate	0.4225	1	0.4225	0.7793	0.3962	
D-HPMC K4M	0.9025	1	0.9025	1.66	0.2234	
<b>Residual</b>	5.96	11	0.5421			
<b>Cor Total</b>	57.72	15				

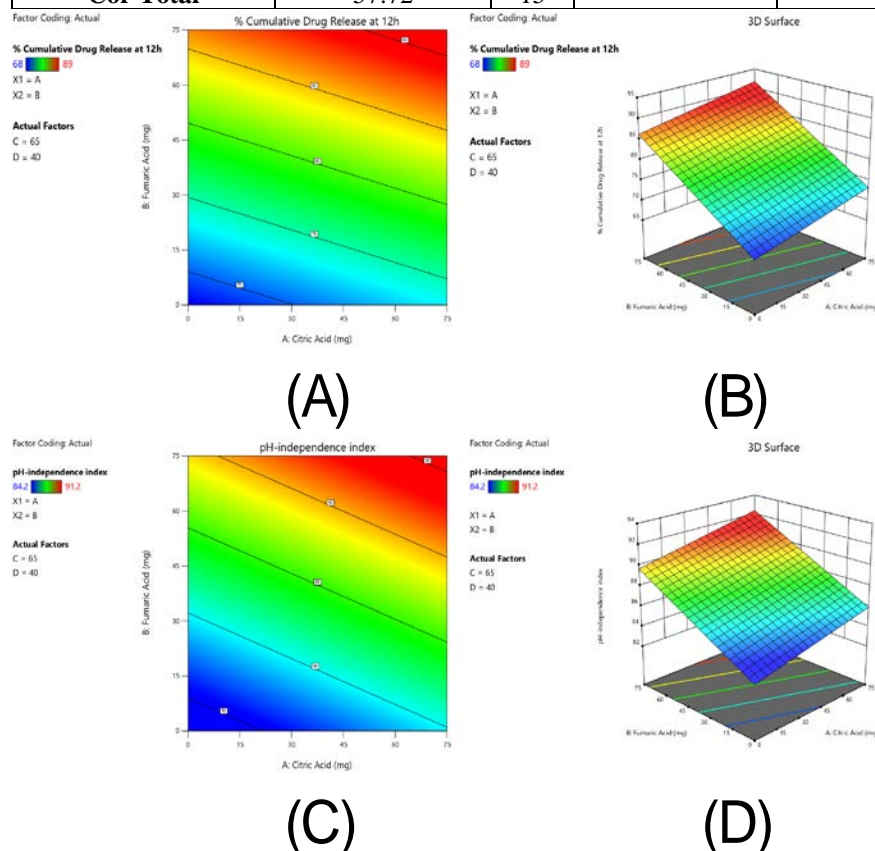


**Figure 3: Contour plots (A, C) and 3D response surface plots (B, D) showing the effects of citric acid and fumaric acid concentrations on (A-B) cumulative drug release at 12h and (C-D) pH-independence index. Red zones indicate optimal formulation regions.**

**Table 10: Validation of Optimized Formulation - Predicted vs Experimental Values**

Batch	Response	Predicted value	Experimental value	% Relative error
F8	% Cumulative Drug Release at 12h	89.463	89	0.52
	pH-independence index	91.313	91.2	0.12

**Table 11: Microenvironmental pH Profile of Formulations During 12-Hour Dissolution Study**

Batch	0 h	0.5 h	1 h	2 h	4 h	6 h	8 h	10 h	12 h
F1	6.80±0.05	6.55±0.08	6.60±0.10	6.65±0.09	6.70±0.08	6.72±0.07	6.75±0.06	6.76±0.05	6.78±0.04
F2	6.80±0.05	3.85±0.18	3.80±0.20	4.20±0.22	4.85±0.25	5.40±0.28	5.85±0.30	6.10±0.25	6.35±0.20
F3	6.80±0.05	3.70±0.20	3.65±0.22	4.05±0.24	4.70±0.27	5.25±0.30	5.70±0.32	5.95±0.28	6.20±0.24
F4	6.80±0.05	3.95±0.16	3.90±0.18	4.30±0.20	4.95±0.23	5.50±0.26	5.95±0.28	6.20±0.23	6.45±0.19
F5	6.80±0.05	3.60±0.22	3.55±0.24	3.95±0.26	4.55±0.28	5.10±0.31	5.55±0.33	5.80±0.29	6.05±0.26
F6	6.80±0.05	4.25±0.17	4.20±0.19	4.55±0.21	5.10±0.24	5.55±0.27	5.95±0.29	6.25±0.24	6.50±0.21
F7	6.80±0.05	4.15±0.19	4.10±0.21	4.45±0.23	5.00±0.26	5.45±0.29	5.85±0.31	6.15±0.27	6.40±0.24
F8	6.80±0.05	4.15±0.14	4.10±0.15	4.25±0.13	4.35±0.16	4.45±0.14	4.50±0.18	4.60±0.20	4.75±0.22
F9	6.80±0.05	4.05±0.16	4.00±0.18	4.15±0.20	4.25±0.22	4.35±0.24	4.45±0.26	4.55±0.28	4.70±0.30
F10	6.80±0.05	3.90±0.17	3.85±0.19	4.25±0.21	4.90±0.24	5.45±0.27	5.90±0.29	6.15±0.25	6.40±0.22
F11	6.80±0.05	3.75±0.21	3.70±0.23	4.10±0.25	4.75±0.28	5.30±0.31	5.75±0.33	6.00±0.29	6.25±0.26
F12	6.80±0.05	4.00±0.15	3.95±0.17	4.35±0.19	5.00±0.22	5.55±0.25	6.00±0.27	6.25±0.23	6.50±0.20
F13	6.80±0.05	3.65±0.20	3.60±0.22	4.00±0.24	4.60±0.26	5.15±0.29	5.60±0.31	5.85±0.27	6.10±0.24
F14	6.80±0.05	4.20±0.16	4.15±0.18	4.50±0.20	5.05±0.23	5.50±0.26	5.90±0.28	6.20±0.24	6.45±0.21
F15	6.80±0.05	4.10±0.18	4.05±0.20	4.40±0.22	4.95±0.25	5.40±0.28	5.80±0.30	6.10±0.26	6.35±0.23
F16	6.80±0.05	4.25±0.14	4.20±0.16	4.55±0.18	5.15±0.21	5.60±0.24	6.05±0.26	6.30±0.22	6.55±0.19
Bulk Medium pH	6.80±0.02	6.72±0.04	6.70±0.03	6.68±0.05	6.65±0.04	6.63±0.06	6.60±0.05	6.58±0.07	6.55±0.06

Data expressed as mean ± SD (n=3). All pH measurements represent

## CONCLUSION

This comprehensive study successfully developed & optimized pH-independent sustained-release matrix tablets of Verapamil HCl using a systematic 2<sup>4</sup> factorial design approach encompassing sixteen formulations. Fumaric acid-based formulation F8 (75 mg fumaric acid, 50 mg HPMC K4M, 80 mg sod. alginate) demonstrated superior performance with 89% drug release at 12 hrs and the highest pH-independence index ( $f_2 = 91.2$ ), significantly outperforming control formulation F1 (72% release,  $f_2 = 85.3$ ). Real-time microenvironmental pH monitoring validated the mechanism, demonstrating that F8 maintained sustained acidification (pH 4.10-4.75) for 12 hours, remaining 2.0-2.5 pH units below the bulk medium pH, thereby ensuring continuous drug solubility despite an alkaline intestinal environment. Citric acid formulations exhibited rapid acid depletion with pH escalating to 6.05-6.45 by 12 hours, while succinic acid formulations showed intermediate behavior, confirming that fumaric acid's low aqueous solubility is critical for sustained microenvironmental pH modification. Drug release kinetic modeling revealed that all formulations best fitted the

Korsmeyer-Peppas model ( $R^2 > 0.99$ ), with F8 exhibiting the lowest release exponent ( $n = 0.512$ ), indicating diffusion-controlled release with minimal erosion.

Statistical optimization identified fumaric acid as the most significant factor (F-value = 26.30,  $p = 0.0003$ ), with model validation showing excellent predictive accuracy (relative error < 0.52%). These findings establish that incorporating fumaric acid into HPMC-alginate matrices represents a simple, cost-effective, and statistically validated strategy for achieving pH-independent sustained release of weakly basic drugs, offering consistent drug release across variations in gastrointestinal pH, reduced dosing frequency, and improved therapeutic outcomes, with significant potential for industrial translation.

## FINANCIAL ASSISTANCE

NIL

## CONFLICT OF INTEREST

The authors declare no conflict of interest.

**AUTHOR CONTRIBUTION**

R U Gaware was responsible for the overall conceptualization and design of the study, formulation of matrix tablets, execution of laboratory experiments, analysis of in vitro release data, and preparation of all tables, figures, and the initial manuscript draft. K Sarvanan provided primary guidance and expert supervision throughout the research process, offering valuable scientific input, protocol optimization strategies, and critical evaluation of experimental results. His role was crucial in shaping the methodology and ensuring scientific accuracy. S L Jadhav contributed to the selection and justification of excipients, the interpretation of dissolution behavior, and assisted in refining the manuscript for academic clarity and technical accuracy. All authors reviewed and approved the final version of the manuscript.

**REFERENCES**

- [1] Thipe SS, Sawale AV, Muneshwar SD, Gulhane SA, Gahukar SS. Formulation and evaluation of buccoadhesive tablet of verapamil hydrochloride for the treatment of hypertension. *J. Drug Deliv. Ther.*, **13**(7), 15-23 (2023) <https://doi.org/10.22270/jddt.v13i7.6122>.
- [2] Grewal S, Singh S, Sharma N, Behl T, Grewal IK, Gupta S. Insights into the pivotal role of calcium channel blockers and its nanoformulations in the management of hypertension. *BioNanoScience*, **13**, 1437-1462 (2023) <https://doi.org/10.1007/s12668-023-01215-w>.
- [3] Ganorkar S, Kulkarni N, Khiste R. A review on recent approaches for the use of different analytical techniques to analyze some calcium channel blockers and their combinations with other antihypertensive drugs. *Curr. Indian Sci.*, **1**(4), E2210299X250401 (2023) <https://doi.org/10.2174/012210299X250401231010114247>.
- [4] Patil AS, Joshi S. Formulation and evaluation of verapamil hydrochloride sustain release tablet. *Res. J. Pharm. Technol.*, **17**(2), 802-806 (2024) <https://doi.org/10.52711/0974-360X.2024.00124>.
- [5] Allaboun H, Alkhamis KA, Al-Nimry SS. Preparation of sustained release formulation of verapamil hydrochloride using ion exchange resins. *AAPS PharmSciTech*, **24**(4), 114 (2023) <https://doi.org/10.1208/s12249-023-02569-w>.
- [6] Adimulapu A, Hussain S, Saripilli R, Jesudasan R. An in-depth analysis of pH-independent controlled drug delivery systems and prospects for the future. *Preprints*, **2024**(8), 2097 (2024) <https://doi.org/10.20944/preprints202408.2097.v1>.
- [7] Chang HHR, Chen K, Lugtu-Pe JA, AL-Mousawi N, Zhang X, Bar-Shalom D, Rantanen J, Bohr A. Design and optimization of a nanoparticulate pore former as a multifunctional coating excipient for pH transition-independent controlled release of weakly basic drugs for oral drug delivery. *Pharmaceutics*, **15**(2), 547 (2023) <https://doi.org/10.3390/pharmaceutics15020547>.
- [8] Shalong MH, Rahman MM, Khan RA, Islam MS. Development of pH-independent sustained release matrix tablets of verapamil hydrochloride using different organic acids. *Int. J. Pharm. Sci. Res.*, **8**(9), 3847-3856 (2017) [https://doi.org/10.13040/IJPSR.0975-8232.8\(9\).3847-56](https://doi.org/10.13040/IJPSR.0975-8232.8(9).3847-56).
- [9] Kumar A, Singh B, Rawal RK, Sharma N. Development and evaluation of pH-independent sustained release matrix tablets of verapamil hydrochloride using natural polymer. *Asian J. Pharm. Clin. Res.*, **11**(6), 245-252 (2018) <https://doi.org/10.22159/ajpcr.2018.v11i6.25289>.
- [10] Kumar R, Patil S, Patil MB, Paschapur MS, Mahalaxmi R. Formulation and evaluation of enteric coated tablets containing HPMCAS as a pore-former and organic acids for pH-independent drug release. *Drug Dev. Ind. Pharm.*, **38**(4), 458-466 (2012) <https://doi.org/10.3109/03639045.2011.608013>.
- [11] Cha KH, Shin SH, Park JH, Choi SC, Park YI, Choi WS, Cho W, Ahn JH, Kim MS, Cho KH, Hwang SJ. pH-independent sustained release tablet using polyethylene oxide and citric acid for weakly basic drug. *Arch. Pharm. Res.*, **34**(9), 1455-1462 (2011) <https://doi.org/10.1007/s12272-011-0911-6>.
- [12] Pooresmaeil M, Javanbakht S, Namazi H, Shaabani A. Application or function of citric acid in drug delivery platforms. *Med. Res. Rev.*, **42**(2), 800-849 (2022) <https://doi.org/10.1002/med.21864>.
- [13] Wang X, Li H, Bao Y, Wang Y, Chen C. Overcoming the application limitations of pH-driven encapsulation of bioactive compounds: strategies and perspectives. *Curr. Opin. Food Sci.*, **59**, 101212 (2024) <https://doi.org/10.1016/j.cofs.2024.101212>.
- [14] Vlad RA, Pinteau A, Pinteau C, Rédei EM, Antonoaea P, Bîrsan M, Ciucă A, Pădureanu V, Olariu S, Ruzs CM, Mureşan ML, Ciurea CN. Hydroxypropyl methylcellulose—a key excipient in pharmaceutical drug delivery systems. *Pharmaceutics*, **17**(6), 784 (2025) <https://doi.org/10.3390/pharmaceutics17060784>.
- [15] Tordi P, Ridi F, Samorì P, Bonini M. Cation-alginate complexes and their hydrogels: a powerful toolkit for the development of next-generation sustainable functional materials. *Adv. Funct. Mater.*, **35**(1), 2416390 (2025) <https://doi.org/10.1002/adfm.202416390>.
- [16] Marchetti L, Truzzi E, Rossi MC, Benvenuti S, Cappelozza S, Saviane A, Bertelli D. Alginate-based carriers loaded with mulberry (*Morus alba* L.) leaf extract: a promising strategy for prolonging 1-deoxyxojirimycin (DNJ) systemic activity for the nutraceutical management of hyperglycemic conditions. *Molecules*, **29**(4), 797 (2024) <https://doi.org/10.3390/molecules29040797>.
- [17] Veronica N, Heng PWS, Liew CV. Alginate-based matrix tablets for drug delivery. *Expert Opin. Drug Deliv.*, **20**(1), 115-130 (2023) <https://doi.org/10.1080/17425247.2023.2158183>.

- [18] Dhondt J, Bertels J, Kumar A, Van Hauwermeiren D, Ryckaert A, Van Snick B, Vanhoorne V, Vercruyssen J, De Beer T, Remon JP, Vervaet C. A multivariate formulation and process development platform for direct compression. *Int. J. Pharm.*, **623**, 121962 (2022) <https://doi.org/10.1016/j.ijpharm.2022.121962>.
- [19] Fayed MH, Aldawsari MF, AlAli AS, Alsaqr A, Almutairy BK, Aodah AH, Alshehri S, Shakeel F. Design-of-experiment approach to quantify the effect of nano-sized silica on tableting properties of microcrystalline cellulose to facilitate direct compression tableting of binary blend containing a low-dose drug. *J. Drug Deliv. Sci. Technol.*, **68**, 103127 (2022) <https://doi.org/10.1016/j.jddst.2022.103127>.
- [20] Canh Pham E, Vo Van L, Viet Nguyen C, Nguyen Duong NT, Le Thi TV. Formulation development, optimization, in vivo antidiabetic effect and acute toxicity of directly compressible herbal tablets containing *Merremia tridentata* (L.) extract. *J. Drug Deliv. Sci. Technol.*, **84**, 104445 (2023) <https://doi.org/10.1016/j.jddst.2023.104445>.
- [21] K S, B D. Design and evaluation of Vildagliptin matrix tablets by response surface methodology. *SSRN Electron. J.*, **4307042** (2022) <https://doi.org/10.2139/ssrn.4307042>.
- [22] Balla TB, Joseph NM, Belete A. Optimization of pregelatinized Taro Boloso-I starch as a direct compression tablet excipient. *BioMed Res. Int.*, **2023**, 9981311 (2023) <https://doi.org/10.1155/2023/9981311>.
- [23] Caccavo D, Iannone M, Barba AA, Lamberti G. Impact of drug release in USP II and in-vitro stomach on pharmacokinetic: the case study of immediate-release carbamazepine tablets. *Chem. Eng. Sci.*, **267**, 118371 (2023) <https://doi.org/10.1016/j.ces.2022.118371>.
- [24] Qiu Y, Zhu DA, Apfelbaum K, Zu H, Xiong H. Development of an in vitro drug release method to enable in vitro–in vivo correlation of potassium chloride extended-release tablets. *Mol. Pharm.*, **19**(11), 4191-4198 (2022) <https://doi.org/10.1021/acs.molpharmaceut.2c00568>.
- [25] Vrbanc H, Trontelj J, Osojnik A, Berginc K, Janković B. Effect of gastrointestinal transit on micro-environmental pH inside HPMC matrix tablets — in vitro study. *Int. J. Pharm.*, **604**, 120718 (2021) <https://doi.org/10.1016/j.ijpharm.2021.120718>.
- [26] Lin JT, Chiang YC, Li PH, Chiang PY. Structural and release properties of combined curcumin controlled-release tablets formulated with chitosan/sodium alginate/HPMC. *Foods*, **13**(13), 2022 (2024) <https://doi.org/10.3390/foods13132022>.
- [27] Zhang Z, Chen S, Wen M, He H, Zhang Y, Yin T, Tang X. Alleviating the influence of circadian rhythms and drug properties to the release of paliperidone gel matrix tablets with compression coating technology and microenvironment shaping. *AAPS PharmSciTech*, **23**(7), 228 (2022) <https://doi.org/10.1208/s12249-022-02388-5>.
- [28] Haznar-Garbacz D, Hoc D, Garbacz G, Lachman M, Słomińska D, Romański M. Dissolution of a biopharmaceutics classification system class II free acid from immediate release tablets containing a microenvironmental pH modulator: comparison of a biorelevant bicarbonate buffering system with phosphate buffers. *AAPS PharmSciTech*, **23**(6), 203 (2022) <https://doi.org/10.1208/s12249-022-02310-z>.
- [29] Zhang S, Xu X, Sun W, Zhang Z, Pan B, Hu Q. Enteric and hydrophilic polymers enhance dissolution and absorption of poorly soluble acidic drugs based on micro-environmental pH-modifying solid dispersion. *Eur. J. Pharm. Sci.*, **168**, 106074 (2022) <https://doi.org/10.1016/j.ejps.2021.106074>.
- [30] Kriangkrai W, Puttipipatkachorn S, Sriamornsak P, Sungthongjeen S. Design and evaluation of new gel-based floating matrix tablets utilizing the sublimation technique for gastroretentive drug delivery. *Gels*, **10**(9), 581 (2024) <https://doi.org/10.3390/gels10090581>.
- [31] Younes NF, El Assasy AEHI, Makhoulf AIA. Microenvironmental pH-modified Amisulpride-Labrasol matrix tablets: development, optimization and in vivo pharmacokinetic study. *Drug Deliv. Transl. Res.*, **11**(1), 103-117 (2021) <https://doi.org/10.1007/s13346-019-00706-2>.
- [32] Maghsoodi M, Asghari F, Nokhodchi A. New insight into acidifier-induced enhancement of dissolution of weakly basic drug, dipyridamole. *J. Pharm. Innov.*, **18**(4), 1626-1637 (2023) <https://doi.org/10.1007/s12247-023-09730-9>.
- [33] Liu Z, Shi C, Fang Y, Zhao H, Mu Y, Zhao L, Feng N. A comprehensive understanding of disintegrants and disintegration quantification techniques: from the perspective of tablet microstructure. *J. Drug Deliv. Sci. Technol.*, **88**, 104891 (2023) <https://doi.org/10.1016/j.jddst.2023.104891>.
- [34] Cai Z, Liu B, Zeng H, Zhang Y, Yin T, He H, Tang X. Sustained-release tablets prepared by compression coating technology achieve similar drug release to osmotic pump tablets: process parameters and in vitro-in vivo evaluation. *J. Drug Deliv. Sci. Technol.*, **111**, 107178 (2025) <https://doi.org/10.1016/j.jddst.2025.107178>.
- [35] Dvořáčková K, Doležel P, Mašková E, Muselík J, Kejdušová M, Vetchý D. The effect of acid pH modifiers on the release characteristics of weakly basic drug from hydrophilic-lipophilic matrices. *AAPS PharmSciTech*, **14**, 1341-1348 (2013) <https://doi.org/10.1208/s12249-013-0019-1>.
- [36] Maskova E, Kubova K, Vyslouzil J, Pavloková S, Vetchy D. Influence of pH modulation on dynamic behavior of gel layer and release of weakly basic drug from HPMC/wax matrices, controlled by acidic modifiers evaluated by multivariate data analysis. *AAPS PharmSciTech*, **18**(4), 1242-1253 (2017) <https://doi.org/10.1208/s12249-016-0588-x>.
- [37] Cha KH, Shin SH, Park JH, Choi SC, Park YI, Choi WS, Cho W, Ahn JH, Kim MS, Cho KH, Hwang SJ. pH-independent

- sustained release tablet using polyethylene oxide and citric acid for weakly basic drug. *Arch. Pharm. Res.*, **34(9)**, 1455-1462 (2011) <https://doi.org/10.1007/s12272-011-0911-6>.
- [38] López-Porfiri P, Gorgojo P, González-Miquel M. Solubility study and thermodynamic modelling of succinic acid and fumaric acid in bio-based solvents. *J. Mol. Liq.*, **369**, 120836 (2023) <https://doi.org/10.1016/j.molliq.2022.120836>.
- [39] Sohn JS, Kim JS, Choi JS. Development of a naftopidil-chitosan-based fumaric acid solid dispersion to improve the dissolution rate and stability of naftopidil. *Int. J. Biol. Macromol.*, **176**, 520-529 (2021) <https://doi.org/10.1016/j.ijbiomac.2021.02.096>.
- [40] Pu YE, Menger R, Tong Z, Gaebale T. Development of an enhanced formulation to minimize pharmacokinetic variabilities of a weakly basic drug compound. *Pharm. Dev. Technol.*, **27(4)**, 406-413 (2022) <https://doi.org/10.1080/10837450.2022.2070206>.
- [41] Wu H, Ma J, Qian S, Jiang W, Liu Y, Li J, Zhang J. Co-amorphization of posaconazole using citric acid as an acidifier and a co-former for solubility improvement. *J. Drug Deliv. Sci. Technol.*, **80**, 104136 (2023) <https://doi.org/10.1016/j.jddst.2022.104136>.
- [42] Siraj EA, Mulualem Y, Molla F, Yayehrad AT, Belete A. Formulation optimization of furosemide floating-bioadhesive matrix tablets using waste-derived Citrus aurantifolia peel pectin as a polymer. *Sci. Rep.*, **15(1)**, 16704 (2025) <https://doi.org/10.1038/s41598-025-95732-1>.
- [43] Streubel A, Siepmann J, Bodmeier R. Drug delivery to the upper small intestine window using gastroretentive technologies. *Curr. Opin. Pharmacol.*, **6(5)**, 501-508 (2006) <https://doi.org/10.1016/j.coph.2006.04.007>.